

## An adaptive flexible polishing path programming method of the blisk blade using elastic grinding tools<sup>†</sup>

Wenbo Huai<sup>1,\*</sup>, Yaoyao Shi<sup>2</sup>, Hong Tang<sup>2</sup> and Xiaojun Lin<sup>2</sup>

<sup>1</sup>*School of High Vocational Education, Xi'an University of Technology, Xi'an, 710082, China*

<sup>2</sup>*School of Mechanical Engineering, Northwestern Polytechnical University, Xi'an, 710072, China*

(Manuscript Received January 22, 2019; Revised March 25, 2019; Accepted March 28, 2019)

### Abstract

As for blisk blade profile polishing, the “five-axis numerical control + flexible grinding head + elastic grinding tool” polishing process equipment has advantages of high precision, little interference, good adaptivity, etc.; in order that the elastic grinding tool (abrasive cloth wheel) can effectively fit in with the blade profile in the polishing process and polishing quality and efficiency can be improved, a polishing path programming method of the elastic grinding tool was studied, feed mode of the elastic grinding tool and parametric method of the blade profile were proposed, and calculation methods of offset surface, polishing spacing, polishing step size and cutter-axis vector were given; this polishing path programming method makes it possible for the flexible spindle mechanism keeps a reasonable pose during the polishing process so that the elastic grinding tool can not only effectively fit in with the blade profile but also the polishing force direction of the elastic grinding tool is basically identical with normal vector direction of the polishing point; the polishing test results indicate that: After polishing, blade surface roughness is smaller than 0.4  $\mu\text{m}$  and blade profile tolerance is within the tolerance zone, thus satisfying technical requirements and indicating that the technology proposed in this paper can satisfy blisk blade profile polishing requirements.

*Keywords:* Blisk; Flexible polishing; Path programming; Elastic grinding tool

### 1. Introduction

As a new-type structural member designed for high-performance aviation engines, blisk has been extensively applied to military and civil aviation aircraft engines in various countries as a key component of aviation engines by virtue of its light weight and high pneumatic rate. Nowadays multi-axis linkage milling process has been mostly used in China, which has already satisfied blisk machining requirements [1]. However, the blisk after milling is a spatial free-form surface with obvious milling scallop height and crest and trough it forms [2], and consequently, the surface roughness is large. Aviation engine blades with disqualified surface roughness will easily experience fatigue failure, deformation or fracture under high-temperature and high-pressure environment [3], and the consequence is unbearable. Therefore, it's necessary to remove a small margin using the polishing technology in order to obtain the surface roughness meeting technical requirements [4], improve fatigue resistance and surface friction performance of the blisk [5] and then improve performance and service life of

aviation engines.

However, as the blisk is of complicated structure, the following difficulties are mainly faced in the process of implementing the automatic polishing technology: (1) Blisk blade is thin, crangle ratio is large, blade span is long, blade spacing is small and openness is poor [2], and as a result, reachability of the grinding tool is poor and machining interference between grinding tool and workpiece can easily occur; (2) the blade is thin with poor rigidity, machining deformation can be easily generated, which will affect surface quality and profile precision [6], and thus higher requirements have been proposed for the flexibility of the grinding tool; (3) machined and formed blade surface has nonuniform margins with severe tool marks and large scallop height between lines and large waviness [7], which puts forward strict requirements for adaptivity of the polishing process system and selection of process parameters; (4) as the blisk plays a significant role in guaranteeing safe and reliable engine operation, requirements for qualified polishing quality indexes are extremely rigorous [8], for instance, machined profile precision should be lower than 0.08 mm and machined surface roughness should be smaller than 0.4  $\mu\text{m}$ , etc. [2].

At present robot [9-11] and numerically-controlled machine tool [12-14] have been extensively used as polishing tools

\*Corresponding author. Tel.: +86 29 88492851, Fax.: +86 29 88492851

E-mail address: huaiwb@xaut.edu.cn

<sup>†</sup>Recommended by Associate Editor Seok-min Kim

© KSME & Springer 2019

both home and abroad. Ideal polishing effect on complex surfaces has been achieved by combining path programming, visual positioning and other technologies; however, numerically-controlled machine tool is of high price [15] without detection function of polishing force and control function [12], and robot polishing path error is large [10]. In terms of grinding tools, PAN et al. polished spherical lens and ZENG and BLUNT [16] polished medical Co-Cr alloy. Gasbag taken as the polishing tool, ideal polishing effects have been realized through a reasonable control of process parameters. As for complicated geometrical shapes, non-contact polishing processes [17–20] like magnetofluid, electrofluid and abrasive fluid have been proposed in the academic circles, but material removal rate and polishing efficiency [17] are low with poor consistency of surface quality and high cost [21]. With a high polishing efficiency, abrasive belt [12, 22, 23] has been used as the main polishing tool, but as the grinding head mechanism is large in volume, it's difficult to enter the blisk with narrow inlet and exhaust passage for polishing [24, 25].

Therefore, Northwestern Polytechnical University has independently developed the “five-axis numeral control + flexible grinding head + elastic grinding tool (abrasive cloth wheel)” polishing process equipment [1, 22]. This equipment features high path precision and favorable adaptivity, and moreover, the abrasive cloth wheel of the grinding tool features small volume and good elasticity under high-speed revolution, so it is applicable to polishing of the blisk blade [23, 24]. Hence, based on structural features of the blisk blade, a flexible polishing path programming method for the elastic grinding tool abrasive cloth wheel was proposed in this paper, and its reliability was verified through test results.

## 2. “Five-axis numerical control + flexible grinding head + elastic grinding tool” polishing process

The structure of the five-axis numerically controlled polishing lathe is shown in Fig. 1. This lathe includes 3 linear motion axes X, Y and Z, 1 blisk rotation axis C and 1 swing axis A of flexible grinding head; the key component of the equipment namely spindle head A of the flexible grinding tool is distributed with 3 micrometric displacement cylinders along the radial direction and installed with 1 micrometric displacement cylinder along the axial direction. In the polishing process, multiple displacement sensors distributed in radial direction and axial direction conduct real-time detection of pose change of the spindle tool. The acquired data signals are input into the industrial control system and calculated through the control algorithm in this system, control signals are output then so that air cylinders execute their actions and flexible spindle A does micrometric displacement action according to the geometric profile change of the blade, and the flexible spindle pose is adjusted in a real-time way so that the abrasive cloth wheel of the elastic grinding tool keeps fitting in with the geometric profile of the blade so as to realize adaptive flexible polishing [1, 22].

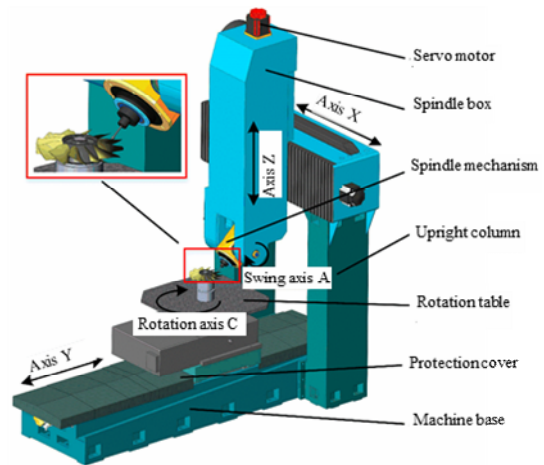


Fig. 1. Five-axis numerically controlled polishing lathe.

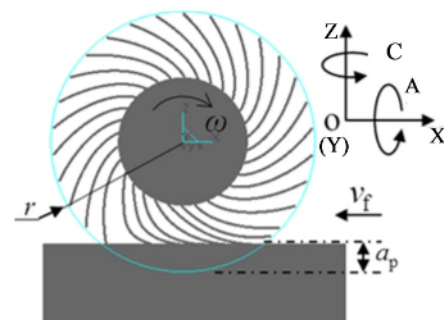


Fig. 2. Polishing principle of abrasive cloth wheel.

Compared with grinding tools such as abrasion wheel and abrasive belt, the abrasive cloth wheel has simple structure and small volume, it can go deeply into the narrow inlet and exhaust passage for polishing, and it can effectively avoid the interference between grinding tool and blade [1, 22–24]; the radius of the abrasive cloth wheel increases under the effect of centrifugal force when revolving at a high speed, great elasticity is generated, and it closely contacts the blade profile in the polishing process, and then a tiny enveloping plane is formed between the surface and abrasive cloth wheel so as to realize “micro-surface tangent contact”, which not only enlarges the polishing area, effectively eliminates the scallop height between lines and improves polishing efficiency but also avoids “over-polishing” or “under-polishing phenomenon caused by rigid grinding heads like abrasion wheel [22–24]. As shown in Fig. 2, polishing process parameters of the abrasive cloth wheel include [1]: Rotate speed ( $\omega / \text{r} \cdot \text{min}^{-1}$ ), compression depth ( $a_p / \text{mm}$ ), feed rate ( $v_f / \text{mm} \cdot \text{min}^{-1}$ ), line spacing ( $p / \text{mm}$ ) and abrasive size  $P$ .

## 3. Polishing path programming method of the elastic grinding tool (abrasive cloth wheel)

NC polishing CL (cutter location) path programming is the key and basis for NC polishing [26, 27]. The machined sur-

face should have favorable surface consistency with uniform polishing patterns and the grinding tool must fit well in with the machined surface in order to avoid “over-polishing” or “under-polishing” and improve machining efficiency [28]. Polishing CL path can be divided into polishing PL (point location) path and cutter axis vector; polishing PL is coordinate data used to accurately mark spatial position of the polishing cutter in the polishing process while cutter axis vector is the vector used to determine the direction of the polishing cutter in the polishing process [26]. During the polishing process, the geometric center of the abrasive cloth wheel can be taken as the polishing PL while the axial direction of its spindle head can be taken as the cutter axis vector direction as shown in Fig. 3.

Path generation methods commonly used in NC programming include cross section method, projection method, parameter line method, equal scallop height method, etc. [29, 30]. Parameter line method, which is the most fundamental cutter path generation method, has been extensively applied to NC programming of all kinds of surface parts by virtue of its advantages: Simple algorithm and small calculated quantity [30]. Therefore, parameter line method is selected in this paper as the polishing path generation algorithm of the blisk blade profile.

Parameter line method generates the cutter path by taking the parameter line as the cutter location point curve, and the surface to be polished is generally taken as the parametric surface. The blisk blade profile is polished, cutter location point path is generated on the offset surface of the blade profile, so offset is needed only after parameterization of the blade profile, and then cutter location point surface is obtained, and cutter location path is generated on the offset surface; in addition, before the path generation, the feed mode should also be determined according to blade structure and actual polishing effect so as to determine basic path line direction and cutter axis vector. To sum up, the cutter location path programming process of the blisk blade profile can be largely divided into: Determination of feed mode, parameterization of the blade profile, generation of the offset surface, determination of polishing spacing and step size as well as cutter axis vector. Fig. 4 shows the polishing cutter location path generated on the blisk blade profile.

### 3.1 Feed modes

The blisk blade has a very high requirement for surface quality. In order to improve fatigue strength of the blade, stress concentration phenomenon should be avoided, the profile surface roughness must be smaller than  $0.4 \mu\text{m}$  and there should be no obvious polishing traces [23]. Different from polishing of die-type free surfaces, as for blade profile polishing, regional division can't be implemented according to indexes like distortion degree; the reason lies in that after the polishing by regions, polishing traces at boundaries between regions can be very obvious, which will easily cause stress

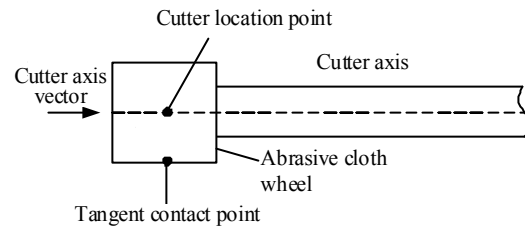


Fig. 3. Cutter location point and cutter axis vector of the abrasive cloth wheel.

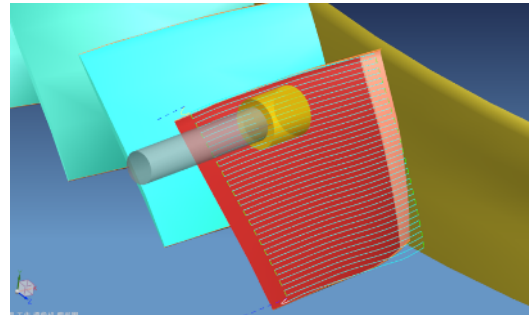


Fig. 4. Polishing cutter location path on the blisk blade profile.

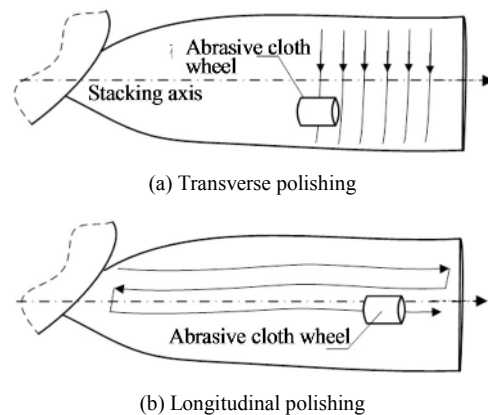


Fig. 5. Feed modes.

concentration; meanwhile, the polishing path should be kept smooth and continuous as far as possible so as to avoid polishing traces caused by sudden change of the cutter axis vector. Therefore, there are two polishing methods suitable for blade profile, namely transverse polishing and longitudinal polishing [24]. The axis of the abrasive cloth wheel is along the blade length (stacking axis) direction in both methods. The abrasive cloth wheel under transverse polishing is polished along the direction of blade milling path, which can effectively remove crest and trough, relative motion direction is along the blade width direction and the polishing efficiency is high as shown in Fig. 5(a); however, the abrasive cloth wheel under longitudinal polishing is polished along the direction perpendicular to the blade milling path, relative motion direction is along the blade length direction and the polishing efficiency is low as shown in Fig. 5(b). Hence, transverse polishing is adopted under general circumstances.

### 3.2 Parameterization of the blade profile

After cutted by the inner hub, the actual blade profile is no longer a complete parametric surface because it's parameters become smaller as shown in Fig. 6(a). If polishing path programming is still conducted according to the parametric surface in the blade shape construction, the generated cutter path will not change with the shape of the blade surface when approaching the blade root, and interference can be easily caused in the polishing process. Therefore, it's usually necessary to do re-parameterization of the blade profile surface and reconstruct its parametric characteristics so that it has uniform parameters as shown in Fig. 6(b).

$c_0$  is set as the air inlet boundary line of the blade profile;  $c_1$  is the exhaust boundary line;  $c_2$  is blade tip boundary line;  $c_3$  is blade root boundary line. Re-parameterization of the blade back surface taken as an example, re-parameterization steps will be herein introduced:

Step 1:  $c_2$  and  $c_3$  are discretized into  $n+1$  points according to the arc length principle, and points along the  $c_0$  direction on  $c_2$  and  $c_3$  are respectively recorded as  $A_i$  ( $i = 0, 1, 2, \dots, n$ ) and  $B_i$  ( $i = 0, 1, 2, \dots, n$ ).

Step 2: Points  $A_i$  and  $B_i$  are connected using a straight line, where  $i = 1, 2, \dots, n-1$  (except for end point), and a cluster of straight lines are obtained as  $l_i$  ( $i = 1, 2, \dots, n-1$ ).

Step 3: Straight lines  $l_i$  ( $i = 1, 2, \dots, n-1$ ) are projected on the blade back surface along the normal direction of the blade back in succession, and the curves after the projection are recorded as  $e_i$  ( $i = 1, 2, \dots, n-1$ ).

Step 4:  $c_0$ ,  $e_i$  ( $i = 1, 2, \dots, n-1$ ) and  $c_1$  are set out and modeled along one direction to generate the surface  $S$ , namely the blade back surface after the re-parameterization. The blade back surface after the re-parameterization has uniform parameters as shown in Fig. 7.

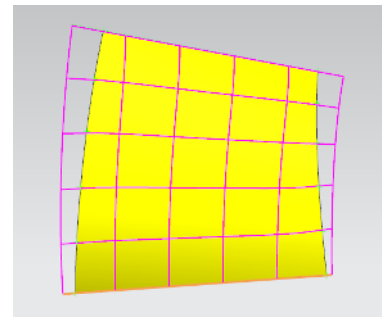
### 3.3 Generation of the offset surface

As polishing point location is the geometric center of the abrasive cloth wheel, but the surface after the parameterization in this paper is a surface where the tangent contact point of the abrasive cloth wheel is located in the polishing process, in order to obtain the cutter location path curve, offset of the blade surface after the parameterization should be carried out as shown in Fig. 8.

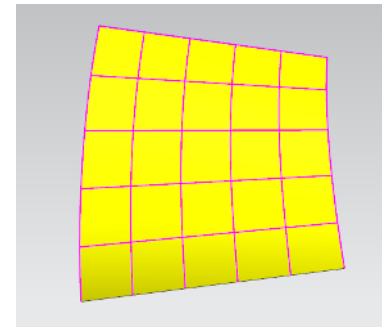
The offset distance is working radius  $R_w$  of the abrasive cloth wheel namely the difference between radius and compression depth ( $r - a_p$ ) when the abrasive cloth wheel is revolving. This offset surface is a surface where the polishing point location is located and where polishing path can be directly generated. The formula of constructing the offset surface of the blade profile is shown in Eq. (1).

$$S(u, v) = s(u, v) + a \cdot N(u, v) \tag{1}$$

where  $S(u, v)$  is equation of the offset surface;  $s(u, v)$  is equa-



(a) The blade back surface after tailoring



(b) Blade back surface after the re-parameterization

Fig. 6. Schematic diagram of the blade surface.

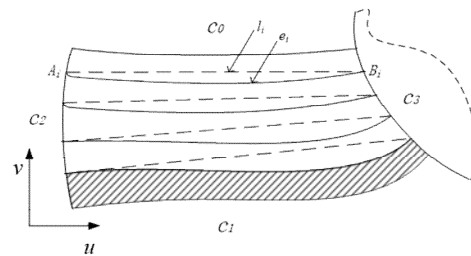


Fig. 7. Schematic diagram of the blade surface re-parameterization.

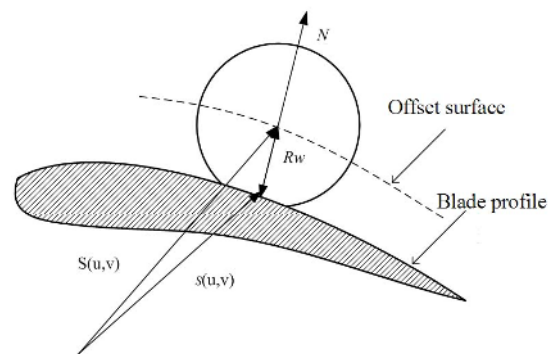


Fig. 8. Blade profile and offset surface.

tion of the polished blade profile surface;  $N(u, v)$  is unit normal vector of the surface  $s(u, v)$ ;  $a$  is normal distance between  $s(u, v)$  and  $S(u, v)$ , and its value is equal to working radius  $R_w$  of the abrasive cloth wheel.

According to the differential geometry theory of the surface, the tangent vector between direction and direction at any point

on the blade profile is shown in Eq. (2).

$$\begin{cases} s_u(u, v) = \frac{\partial s(u, v)}{\partial u} \\ s_v(u, v) = \frac{\partial s(u, v)}{\partial v} \end{cases} \quad (2)$$

The unit normal vector  $N(u, v)$  at this point is shown in Eq. (3).

$$N(u, v) = \frac{s_u(u, v) \times s_v(u, v)}{|s_u(u, v) \times s_v(u, v)|} \quad (3)$$

The equation of the offset surface can be obtained by substituting the unit normal vector into Eq. (1), as shown in Eq. (4).

$$S(u, v) = s(u, v) + R_w \cdot \frac{s_u(u, v) \times s_v(u, v)}{|s_u(u, v) \times s_v(u, v)|} \quad (4)$$

### 3.4 Determination of polishing spacing

Polishing spacing  $p$ , which refers to the distance between two adjacent polishing path lines, directly influences polished surface quality and polishing efficiency. If the spacing is too large, feed times will be reduced, but the engagement effect between lines will be not ideal, and consequently, not only that machining patterns left by milling can't be radically removed but also that obvious polishing traces can be easily generated, which will affect consistency of surface quality; if the spacing is too small, though the polished surface quality can be improved, the polishing efficiency will be greatly reduced. Therefore, reasonable selection of polishing spacing is of great importance to guaranteeing polishing quality and improving polishing efficiency.

In milling and grinding process, equal scallop height method is usually adopted to determine the spacing. However, abrasive cloth wheel polishing is different with an extremely small amount of material removed, actual polishing depth is far smaller than compression depth of the abrasive cloth wheel, so if equal scallop height method is still used to calculate polishing spacing, the quantity of generated path lines will increase, which causes too low polishing efficiency. In order to improve polishing quality and efficiency, polishing spacing is determined according to polishing bandwidth  $D$ ; the experience in actual polishing combined, when the polishing spacing  $p$  is smaller than 1/4 of the polishing bandwidth  $D$  [23, 24] ( $p \leq D/4$ ), the blade profile quality can be guaranteed.

Under the longitudinal polishing mode, the polishing bandwidth is the tangential width of the contact zone between abrasive cloth wheel and workpiece. As curvature radius of the blade is far greater than radius of the abrasive cloth wheel, the blade profile is regarded as a plane for the convenience of calculation, and the geometric relation as shown in Fig. 9 should be satisfied between polishing bandwidth and com-

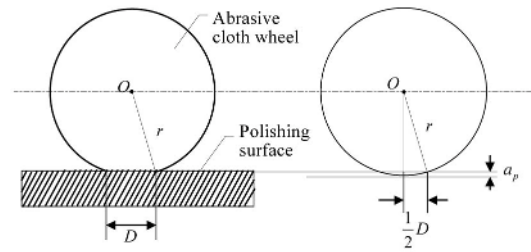


Fig. 9. Schematic diagram of the relationship between polishing bandwidth and compression depth of the abrasive cloth wheel.

pression depth of the elastic grinding tool.

The polishing bandwidth  $D$  can be expressed by Eq. (5) according to Fig. 9.

$$D = 2\sqrt{r^2 - (r - a_p)^2} \quad (5)$$

where  $D$  is polishing bandwidth;  $r$  is radius of the abrasive cloth wheel when revolving;  $a_p$  is compression depth of the abrasive cloth wheel.

If the abrasive cloth wheel of specimens of 8.5 mm × 14 mm/320<sup>#</sup> (initial radius  $r_0$  × thickness  $L$  × abrasive size  $P$ ) is selected, its initial radius is 8.5 mm, and according to Ref. [1], its radius under the rotate speed of 6000 r/min can be obtained as  $r = 10$  mm. According to the polishing experience, deformation of the abrasive cloth wheel is generally within 0.6 mm~1.2 mm. According to Eq. (5), the scope of the polishing bandwidth can be determined as 6.8 mm~9.5 mm, so when the polishing spacing  $p$  is smaller than 1/4 of the polishing bandwidth (1.7 mm~2.3 mm), the blade profile quality can be guaranteed; under the transverse polishing mode, the width  $L$  of the abrasive cloth wheel is approximately equal to its bandwidth  $D$ , namely  $L \approx D = 14$  mm, and then the spacing  $p$  should be smaller than 3.5 mm.

### 3.5 Determination of the polishing step size

The polishing step size is the distance between two adjacent cutter location points on the polishing path line, and usually equal chord height error method [31] is used to calculate the step size as shown in Fig. 10.

In the figure,  $t_i$  and  $t_{i+1}$  are two adjacent tangent contact points on the polishing path, and  $R_i$  and  $R_{i+1}$  are curvature radiuses at the two points respectively. As the two points are adjacent,  $R = R_i = R_{i+1}$  is set for the convenience of calculation.  $l$  is the distance between two adjacent tangent contact points,  $L_a$  is step size,  $\varepsilon$  is the set chord height error, and their geometric relations are shown in Eq. (6).

$$R - \sqrt{R^2 - \left(\frac{l}{2}\right)^2} = \varepsilon \quad (6)$$

Eq. (7) can be obtained through the numerator rationalization in Eq. (6).

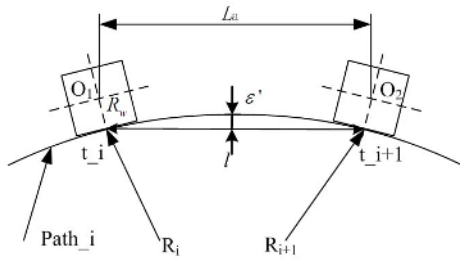


Fig. 10. Schematic diagram of chord height errors.

$$\frac{l^2}{4R(1 + \sqrt{1 - (\frac{l}{2R})^2})} = \epsilon. \tag{7}$$

As  $l \ll R$ ,  $1 + \sqrt{1 - (\frac{l}{2R})^2} \approx 2$ , and then Eq. (7) can be simplified as Eq. (8).

$$\frac{l^2}{8R} = \epsilon. \tag{8}$$

Machining step size  $L_a$  can be expressed by Eq. (9).

$$L_a = \frac{(R \pm R_w)l}{R}. \tag{9}$$

Eq. (10) can be obtained by substituting Eq. (8) into Eq. (9).

$$L_a = \frac{R \pm R_w}{R} \sqrt{8\epsilon R} \tag{10}$$

where curvature radius  $R$  is shown in Eq. (11).

$$R = \frac{|s_u(u, v)|^3}{|s_u(u, v) \times s_{uu}(u, v)|}. \tag{11}$$

In Eq. (10), the value is positive when the surface is convex and it is negative when the surface is concave.

In NC machining, workpiece surface quality is greatly influenced by chord height error [31]. When the chord height error is too high, the material removal rates on the blade surface will be nonuniform so that “over-polishing” occurs. But when it is too small, the calculated quantity will be too large, which causes program bloating. During the blade profile polishing process, as the abrasive cloth wheel is of certain flexibility, the tangent contact status with the blade profile can be automatically adjusted within a certain scope, a value designated in the blade finish-milling process is generally taken as the chord height error, namely  $\epsilon = 0.005$  mm.

### 3.6 Determination of the cutter axis vector

Cutter axis vector is the vector controlling spatial pose of

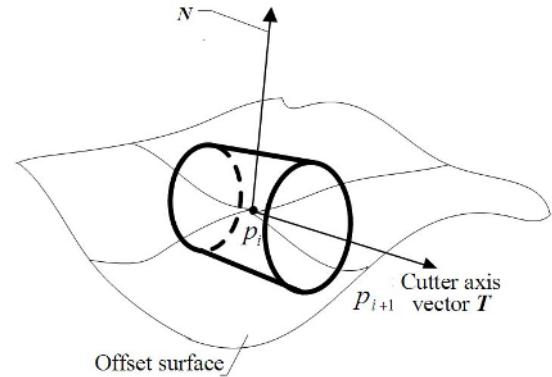


Fig. 11. Cutter axis vector.

the cutter during the polishing process. Different from abrasion belt, abrasive cloth wheel polishing only needs to control its axis vector in order to realize effective tangent contact between the cutter and workpiece under no interference, and reasonable cutter axis vector control can greatly improve consistency of the blade surface quality. During the transverse polishing process, tangent vector direction  $u$  is usually taken as the cutter axis vector direction in order that the polishing force direction can be consistent with the normal vector direction of the polishing point as shown in Fig. 11.

Cutter axis vector is set as  $T$ , and then it can be expressed by Eq. (12).

$$T = s_u(u, v). \tag{12}$$

Eq. (13) can be obtained by substituting it into Eq. (1).

$$T = s_u(u, v) + a \cdot N_u(u, v) \tag{13}$$

where unit normal vector of the contact point can be expressed by Eq. (14).

$$N_u(u, v) = \frac{s_{uv}(u, v) \times [s_v(u, v) - s_u(u, v)]}{|s_u(u, v) \times s_v(u, v)|}. \tag{14}$$

Then the cutter axis vector  $T$  is shown in Eq. (15).

$$T = s_u(u, v) + a \cdot \frac{s_{uv}(u, v) \times [s_v(u, v) - s_u(u, v)]}{|s_u(u, v) \times s_v(u, v)|}. \tag{15}$$

## 4. Polishing test

The test was programed using the polishing path programming method stated in this paper to verify its reliability. Process parameters were selected within the priority intervals [1] of polishing process parameters of the abrasive cloth wheel as shown in Table 1. The polishing test was carried out for two blades (blade back surfaces) numbered as A and B on the blisk at one stage of the engine with material of TC4 on the

Table 1. Polishing parameters.

Parameters	Value	
	Blade A	Blade B
$\omega$ (r · min <sup>-1</sup> )	7500	7000
$p$ (mm)	0.8	1
$a_p$ (mm)	1.2	1
$v_f$ (m · min <sup>-1</sup> )	180	120
$P$	320	400

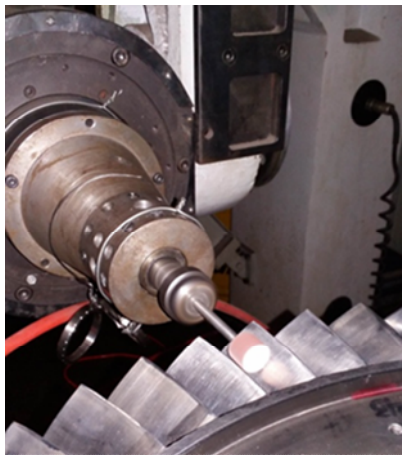


Fig. 12. Polishing test.

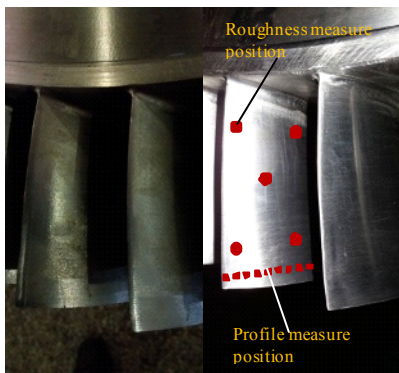


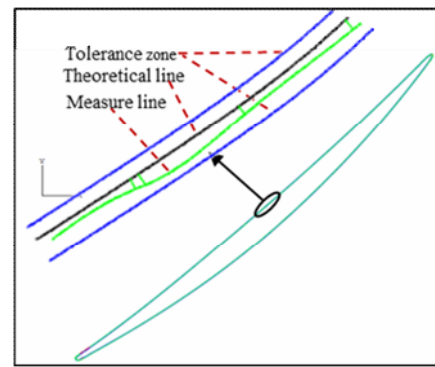
Fig. 13. Comparison of polishing effect.

above mentioned special NC polishing machine in a transverse feed mode as shown in Fig. 12; the abrasive cloth wheel (specifications: 8.5 mm × 14 mm ×  $P$ ) with abrasive particles green silicon carbides was used as the elastic grinding tool.

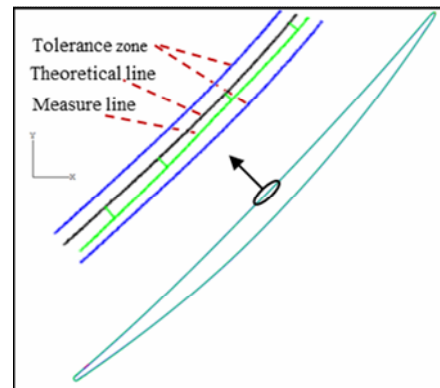
Before and after the polishing, iron slags on the polishing surface should be removed. A portable roughness tester Mar Surf M300C was used to measure roughness values of two blades A and B at the measuring position shown in Fig. 13 by randomly selecting 5 different point locations in the direction perpendicular to the polishing path direction, and the maximum values were taken as measured results; blade tip profile tolerance was measured using a three-coordinate measuring

Table 2. Polishing test results.

Blade	Roughness ( $\mu\text{m}$ )	
	Before polishing	After polishing
A	1.12	0.38
B	1.26	0.37



(a) Blade A



(b) Blade B

Fig. 14. Profile line.

machine.

According to polishing results shown in Table 2, roughness values of two blades A and B satisfy  $R_a < 0.4 \mu\text{m}$  after the polishing, thus satisfying drawing requirements, and the comparison of the blade surfaces before and after polishing is shown in Fig. 13; after the polishing, profile tolerances of both blades A and B will be within the tolerance zone, indicating that the blade profile is not damaged, as shown in Fig. 14; polishing time of blades A and B are about 32 min and 49 min respectively, and about 70 min is needed for artificial polishing of a single blade. Polishing test results of the blisk blade indicate that: the polishing process proposed in this paper effectively reduces surface roughness and guarantees blade profile precision, and the efficiency is obviously improved relative to artificial polishing, thus reducing the labor intensity and verifying that the method proposed in this paper can satisfy blisk blade profile polishing requirements of aviation engines.

## 5. Conclusions

(1) The adaptive flexible polishing principle of the blisk blade polishing process equipment was introduced.

(2) For the polishing process features of the blisk blade, the adaptive flexible polishing path programming method of the blisk blade was given, including determination of feed mode, profile parameterization, generation of offset surface, calculation of polishing spacing, polishing step size and cutter axis vector, etc.

(3) The proposed path programming method makes it possible for the flexible spindle mechanism to keep a reasonable pose in the polishing so as to effectively avoid “under-polishing” and “over-polishing” phenomena. It ensures that the elastic grinding tool can effectively fit in with the blade profile, the polishing force direction is basically identical with the normal vector direction of polishing point locations and then polishing quality and efficiency are improved.

(4) The polishing test proves that the method proposed in this paper can satisfy the blisk blade profile polishing requirements of aviation engines.

## Acknowledgments

This work is supported by the Key Laboratory of Contemporary Design and Integrated Manufacturing Technology Ministry of Education, China.

## Nomenclature

$a_p$	: Compression depth
$\omega$	: Rotate speed
$v_f$	: Feed rate
$p$	: Line spacing
$P$	: Abrasive size
$D$	: Polishing bandwidth
$r$	: Radius of the abrasive cloth wheel
$R_w$	: Processing parameters working radius
$L_a$	: Step size

## References

[1] W. B. Huai, Y. Y. Shi, H. Tang and X. J. Lin, Sensitivity of surface roughness to flexible polishing parameters of abrasive cloth wheel and their optimal intervals, *Journal of Mechanical Science and Technology*, 31 (2) (2017) 865-873.

[2] G. J. Xiao and Y. Huang, Equivalent self-adaptive belt grinding for the real-R edge of an aero-engine precision-forged blade, *International Journal of Advanced Manufacturing Technology*, 83 (9-12) (2016) 1697-1706.

[3] H. Huang, Z. M. Gong and X. Q. Chen, Robotic grinding and polishing for turbine-vane overhaul, *Journal of Materials Processing Technology*, 127 (2) (2002) 140-145.

[4] M. Bigerelle, A. Gautier, B. Hagege and B. Bounichane, Roughness characteristic length scales of belt finished sur-

face, *Journal of Materials Processing Technology*, 209 (20) (2009) 6103-6116.

[5] W. H. Ho, J. T. Tsai, B. T. Lin and J. Chou, Adaptive network-based fuzzy inference system for prediction of surface roughness in end milling process using hybrid Taguchi-genetic learning algorithm, *Expert Systems with Applications*, 36 (2) (2009) 3216-3222.

[6] P. B. Zhao and Y. Y. Shi, Composite adaptive control of belt polishing force for aero-engine blade, *Chinese Journal of Mechanical Engineering*, 26 (5) (2013) 988-996.

[7] G. J. Xiao, Y. Huang and G. L. Chen, Investigations on belt grinding of GH4169 nickel-based superalloy, *Advanced Materials Research*, 1017 (2014) 15-20.

[8] G. J. Xiao, Y. Huang and Y. Yang, Workpiece surface integrity of GH4169 nickel-based superalloy when employing abrasive belt grinding method, *Advanced Materials Research*, 936 (2014) 1252-1257.

[9] Y. Huang, L. Zhang, Z. Huang and Q. Guo, Experimental analysis of the abrasive belt follow-up grinding of Zirconium-4 alloys tubes and pipes, *Journal of Chongqing University*, 35 (10) (2012) 30-37 (in Chinese).

[10] G. L. Wang, Y. Q. Wang, L. Zhang and H. B. Zhou, Development and polishing process of a mobile robot finishing large mold surface, *Machining Science and Technology*, 18 (4) (2014) 603-625.

[11] J. J. Marquez, J. M. Perez, J. J. Rios and A. Vizán, Process modeling for robotic polishing, *Journal of Materials Processing Technology*, 159 (1) (2005) 69-82.

[12] J. Chaves-jacob, J. M. Linares and J. M. Sprauel, Control of the contact force in a pre-polishing operation of free-form surfaces realised with a 5-axis CNC machine, *CIRP Annals-Manufacturing Technology*, 64 (1) (2015) 309-312.

[13] D. H. Zhu, S. Y. Luo, L. Yang and W. Chen, On energetic assessment of cutting mechanisms in robot-assisted belt grinding of titanium alloys, *Tribology International*, 90 (2015) 55-59.

[14] G. J. Xiao and Y. Huang, Constant-load adaptive belt polishing of the weak-rigidity blisk blade, *International Journal of Advanced Manufacturing Technology*, 78 (9-12) (2015) 1473-1484.

[15] R. Pan, Z. Z. Wang, C. J. Wang, Y. H. Xie, D. X. Zhang and Y. B. Guo, Research on control optimization for bonnet polishing system, *International Journal of Precision Engineering and Manufacturing*, 15 (3) (2014) 483-488.

[16] S. Y. Zeng and L. Blunt, Experimental investigation and analytical modelling of the effects of process parameters on material removal rate for bonnet polishing of cobalt chrome alloy, *Precision Engineering*, 38 (2) (2014) 348-355.

[17] Y. Q. Wang, S. H. Yin, H. Huang, F. J. Chena and G. J. Deng, Magnetorheological polishing using a permanent magnetic yoke with straight air gap for ultra-smooth surface planarization, *Precision Engineering*, 40 (1) (2015) 309-317.

[18] E. S. Lee, S. G. Lee, W. K. Choi and S. G. Choi, Study on the effect of various machining speeds on the wafer polishing process, *Journal of Mechanical Science and Technology*,



- 27 (10) (2013) 3155-3160.
- [19] Z. W. Zhong, Recent advances in polishing of advanced materials, *Materials and Manufacturing Processes*, 23 (5) (2008) 449-456.
- [20] M. Givi, A. F. Tehrani and A. Mohammadi, Polishing of the aluminum sheets with magnetic abrasive finishing method, *International Journal of Advanced Manufacturing Technology*, 61 (9-12) (2012) 989-998.
- [21] M. Li, B. H. Lyu, J. L. Yuan, C. C. Donga and W. T. Dai, Shear-thickening polishing method, *International Journal of Machine Tools & Manufacture*, 94 (7) (2015) 88-99.
- [22] W. B. Huai, H. Tang, Y. Y. Shi and X. J. Lin, Prediction of surface roughness ratio of polishing blade of abrasive cloth wheel and optimization of processing parameters, *International Journal of Advanced Manufacturing Technology*, 90 (1) (2017) 699-708.
- [23] J. F. Zhang, Y. Y. Shi, X. J. Lin and Z. S. Li, Five-axis abrasive belt flap wheel polishing method for leading and trailing edges of aero-engine blade, *International Journal of Advanced Manufacturing Technology*, 93 (9-12) (2017) 3383-3393.
- [24] J. F. Zhang, Y. Y. Shi, X. J. Lin and Z. S. Li, Parameter optimization of five-axis polishing using abrasive belt flap wheel for blisk blade, *Journal of Mechanical Science and Technology*, 31 (10) (2017) 4805-4812.
- [25] J. H. Duan, Y. M. Zhang and Y. Y. Shi, Belt grinding process with force control system for blade of aero-engine, *Proceedings of the Institution of Mechanical Engineers Part B-journal of Engineering Manufacture*, 230 (5) (2016) 858-869.
- [26] E. Brinksmeier, O. Riemer and A. Gessenharter, Finishing of structured surfaces by abrasive polishing, *Precision Engineering*, 30 (3) (2006) 325-336.
- [27] Y. Q. Sun, D. J. Giblin and K. Kazerounian, Accurate robotic belt grinding of workpieces with complex geometries using relative calibration techniques, *Robotics and Computer-Integrated Manufacturing*, 25 (1) (2009) 204-210.
- [28] Y. J. Shi, D. Zheng, L. Y. Hu and Y. Q. Wang, NC polishing of aspheric surfaces under control of constant pressure using a magnetorheological torque servo, *International Journal of Advanced Manufacturing Technology*, 58 (9-12) (2012) 1061-1073.
- [29] Z. J. Yang, F. Chen, J. Zhao and X. J. Wu, A novel vision localization method of automated micropolishing robot, *Journal of Bionic Engineering*, 6 (1) (2009) 46-54.
- [30] C. Tournier and E. Duc, A surface-based approach for constant scallop height tool-path generation, *The International Journal of Advanced Manufacturing Technology*, 19 (5) (2002) 318-324.
- [31] C. Walter, M. Rabiey, M. Warhanek and N. Jochum, Dressing and truing of hybrid bonded CBN grinding tools using a short-pulsed fibre laser, *CIRP Annals - Manufacturing Technology*, 61 (1) (2012) 279-282.



**Wenbo Huai** received master's degree in engineering from Xi'an University of Technology in 2009 and doctorate of engineering from Northwestern Polytechnical University in 2018. China. Mr. Huai is currently an Associate Professor at the School of High Vocational Education at Xi'an University of Technology in Xi'an, China. His research fields is adaptive polishing technique for complex surface.